J Therm Anal Calorim (2011) 104:507–513
DOI 10.1007/s10973-011-1336-9

A study of ochres from an Australian aboriginal bark painting using thermal methods

P. S. Thomas · B. H. Stuart · N. McGowan · J. P. Guerbois · M. Berkahn · V. Daniel

Cultural Heritage Special Chapter
© Akadémiai Kiadó, Budapest, Hungary 2011

Abstract The potential of thermogravimetric analysis (TG) as a tool for the characterisation of ochre paint used in indigenous Australian bark paintings has been investigated. TG has been combined with differential scanning calorimetry (DSC) and mass spectrometry (MS) to identify and quantify the main inorganic and organic components present in the paints. The results obtained were supported by comparison with infrared spectra and XRD data obtained for the same specimens. The potential of thermal methods for the characterisation ochres has been demonstrated, with subtle differences between small samples being able to be identified.

Keywords Differential scanning calorimetry · Infrared spectroscopy · Mass spectrometry · Ochre · Painting · Thermogravimetric analysis · X-ray diffraction

Introduction

Bark painting is an important art form in indigenous Australian society [1]. In addition to being culturally significant, such artworks are popular in national and international art collections. The increasing recognition and value of such paintings means that there is an increasing emphasis placed on the characterisation of such artefacts. The establishment of a straightforward means of determining the provenance of bark paintings has the potential to provide valuable information for those concerned with documenting the objects in museum collections and those with an interest in controlling art fraud.

The bark used in indigenous art works of Northern Australia is mainly stripped from the Stringybark (*Eucalyptus teredonta*) tree and heated in fire before use. Traditionally, the main pigments employed were ochres, which come from specific locations around Australia [2]. Modern indigenous paintings commonly use acrylic paints. Traditional binders have included plant liquids such as sap or juice from orchids or turtle egg yolk, while modern bark paintings commonly use acetate or acrylic binders.

The composition of the pigments traditionally used in Australian aboriginal bark paintings has been previously investigated. The elemental and mineral compositions of Australian ochres have been examined using a variety of techniques including X-ray diffraction (XRD) [2–5], proton induced X-ray emission (PIXE) [2, 5], Raman spectroscopy [4, 6], infrared spectroscopy [4, 6], scanning electron microscopy–electron dispersive spectroscopy (SEM–EDS) [2], and inductively coupled plasma mass spectrometry (ICPMS) [2]. Although each of these analytical methods is recognised as a useful tool for the examination of ochre pigments, there are some drawbacks to consider. Both infrared and Raman spectroscopy are useful for identifying paint components, but are more limited when attempting to investigate the regional variation of ochres. ICPMS, SEM–EDS, and PIXE all provide elemental information, but cannot provide phase information and synchrotron radiation. XRD has provided valuable

P. S. Thomas · B. H. Stuart (✉) · N. McGowan
Department of Chemistry and Forensic Sciences, University of Technology, Sydney, PO Box 123, Broadway, NSW 2007, Australia
e-mail: Barbara.Stuart@uts.edu.au

J. P. Guerbois · M. Berkahn
Faculty of Science, University of Technology, Sydney, PO Box 123, Broadway, NSW 2007, Australia

V. Daniel
Australian Museum, 6 College Street, Sydney, NSW 2010, Australia

information about ochre phase analysis and composition, but is limited to crystalline phases and phases that are fairly prominent (>1%) and, for synchrotron XRD, currently there is limited access to beam time and reactors to carry out such studies.

The aim of the current study was to investigate the potential of thermal analysis as an approach to the characterisation of ochres used in bark paintings. Thermogravimetric analysis (TG) combined with differential scanning calorimetry (DSC) and mass spectrometry (MS) has been used to examine paint obtained from an indigenous bark painting provided by the Australian Museum in Sydney. XRD and Fourier transform infrared (FTIR) spectroscopy have also been used in this study for comparison purposes.

Materials and methods

Paint specimens

The painting used for this study is part of a reference collection held by the Australian Museum. The painting is illustrated in Fig. 1 and contains regions showing four different pigment colours. Small quantities of paint specimens were obtained from the painting using tweezers and spatula. Paint was obtained from black, pink, brown, and cream regions.

FTIR spectroscopy

Powdered specimens were mixed with KBr in a 1:100 mass ratio and pressed with 10 ton in.$^{-2}$ pressure to produce discs. Mid-infrared spectra were recorded using Digilab/Varian FTS7000 FTIR spectrometer using a resolution of 4 cm^{-1} averaged over 256 scans.

X-ray diffraction

XRD patterns of the paint specimens were recorded with a Siemens D5000 X-ray diffractometer using Cu K_α radiation. Diffraction patterns were collected over a range of $2\theta = 4°–85°$ at 0.02° steps using a 2.5-s acquisition time per step.

Thermal analysis

The samples were examined by TG–DSC–MS using a Setaram Setsys 16/18 thermobalance coupled with a Balzers ThermoStar mass spectrometer for evolved gas analysis (EVA). Experiments were carried out by placing 20 ± 1 mg of sample into a platinum crucible and heating at a rate of 5 °C/min from ambient temperature to 1000 °C in oxidising (instrument grade air supplied by BOC Australia) and non-oxidising (high purity argon supplied by BOC Australia, rated at <10 ppm O_2) atmospheres at a flow rate of 20 mL/min. Temperature calibration was carried out using indium, tin, aluminium, gold, and silver. Baseline curves were measured under the same experimental conditions in order to account for the effects of purge gas flow and buoyancy on the balance. The peaks in the mass spectra chosen for analysis were at 12, 18, 28, 29, 30, 32, 44, 48, 54, 64, 66, 67, 70, 72, 78, 81, and 91 amu with an aim to identify the presence of water, CO_2, SO_2, organic compounds, and charcoal.

Results

FTIR spectroscopy

The FTIR spectra of the paint specimens are shown in Fig. 2. The spectra are dominated by the spectrum of kaolinite [7, 8]. The spectra of clays are, however, strongly

Fig. 1 Photograph of Aboriginal bark painting

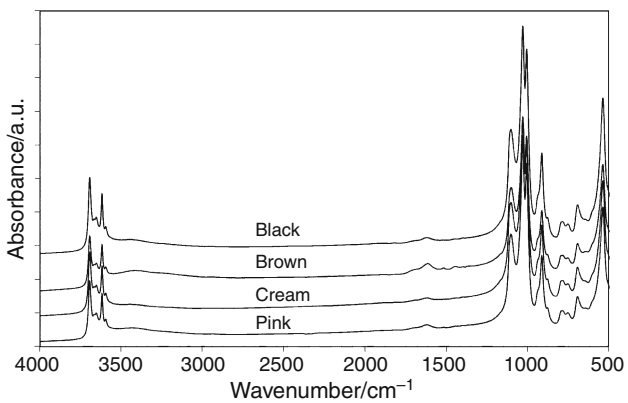

Fig. 2 FTIR spectra of paint specimens

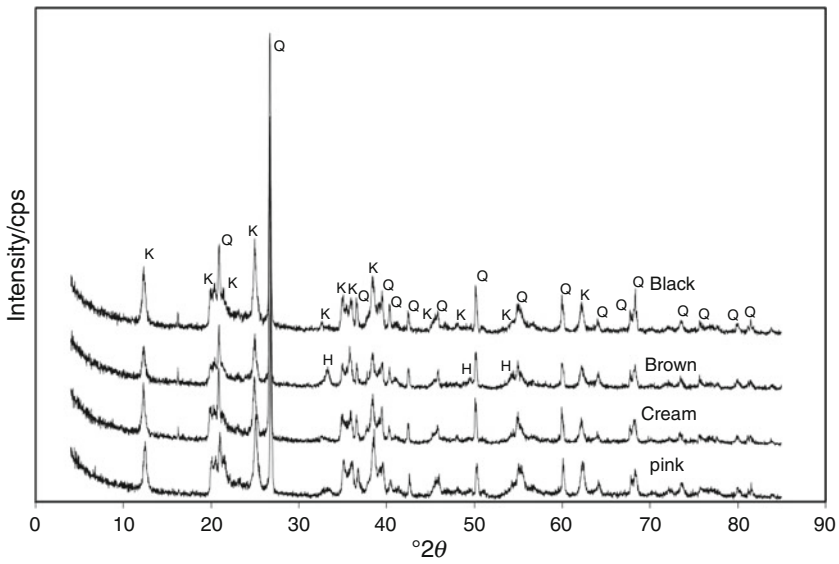

Fig. 3 XRD patterns of paint specimens

dependent on the stacking and defect structures of the clay [7]. The spectrum is also affected by ion substitution through weathering processes [9]. The strong similarity between the spectra in the 600–1000 cm^{-1} range suggests that the peaks present are associated with the clays rather than other impurities (or colorants added) such as goethite or haematite. The increased intensity of the peak at around 790 cm^{-1} suggests the presence of dickite in the kaolinite. The peak at 882 cm^{-1} is characteristic of Fe^{3+} substitution in for octahedral Al^{3+}. Closer inspection of the peak at 790 cm^{-1} reveals the presence of a two peaks at 780 and 793 cm^{-1}. The presence of the peak at 793 cm^{-1} may be indicative of goethite, as this mineral is reported to have two peaks at 796 and 892 cm^{-1} [10]. However, these peaks are expected to be accompanied by a series of peaks at 1344, 1502, and 1624 cm^{-1}, but here are absent or dominated by other strong peaks. It is also possible that the two peaks at 780 and 795 cm^{-1} indicate the presence of quartz [11]. The series of peaks observed in the region 1500–1800 cm^{-1} (at 1442, 1516, 1612, and 1691 cm^{-1}) correlate with the reported spectra of wood charcoal [12]. Significant aromatic characteristics are evidenced by the presence of the strongest peak at 1612 cm^{-1}. These organic peaks are observed in all of the samples, but are most intense in the brown pigment.

X-ray diffraction

The XRD patterns for the four paint specimens are shown in Fig. 3. The XRD data confirm the presence of kaolinite (JCPDS file 01-078-2110 (C)) in each case. Quartz (JCPDS file 00-046-1045 (*)) is also observed to be present. The kaolinite and the quartz dominate the diffraction pattern, but some of the peaks observed are not accounted for by these phases. The diffraction patterns for haematite (JCPDS file 01-089-8103 (C)) and iron oxide hydroxide (JCPDS file 01-076-0182 (C)) both correspond to these remaining peaks. As the peaks are weak in intensity and broad, a positive identification of the iron oxide/hydroxide phase is not possible. The haematite/iron oxide hydroxide

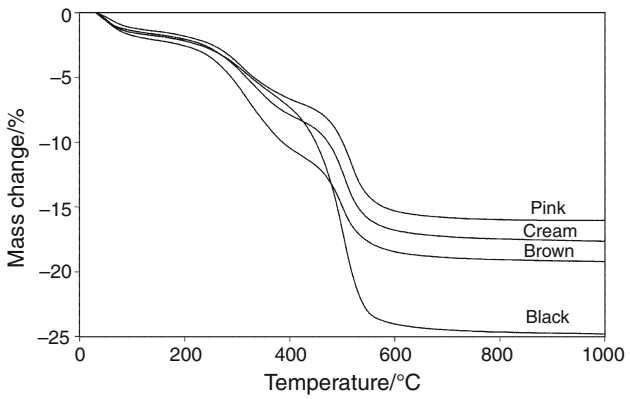

Fig. 4 TG data for paint specimens in an air atmosphere

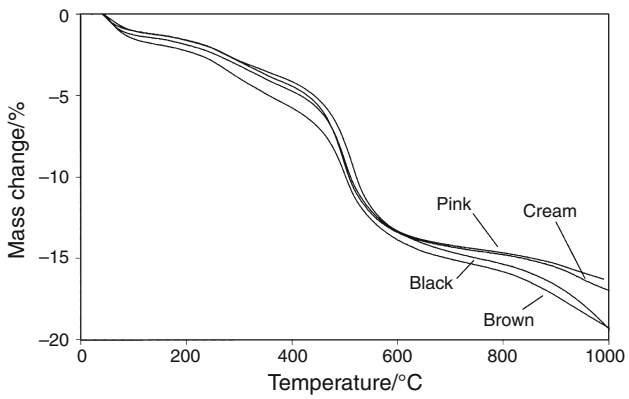

Fig. 5 TG data for paint specimens in an argon atmosphere

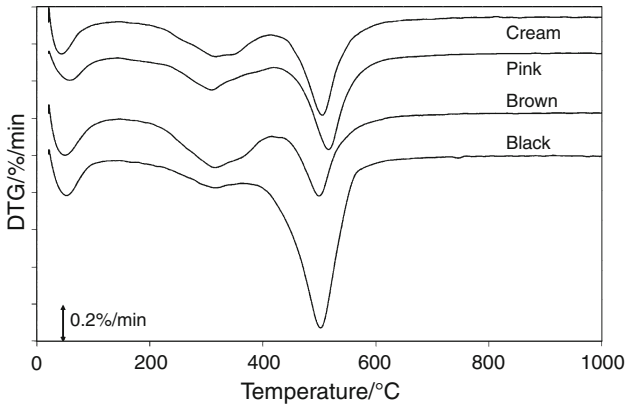

Fig. 6 DTG data for paint specimens in an air atmosphere

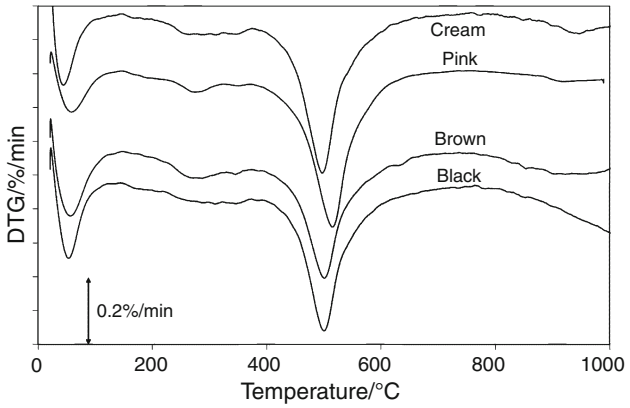

Fig. 7 DTG data for paint specimens in an argon atmosphere

phase is most intensely observed in the brown pigment, with decreasing intensity in the pink and cream phases, and is absent in the black pigment.

Thermal analysis

TG–DSC–MS was carried out in both oxidising (air) and non-oxidising (argon) atmospheres. The TG curves are shown in Figs. 4 and 5, and the DTG curves in Figs. 6 and 7, respectively. The aim of using both inert and oxidising atmospheres was to differentiate the presence of coals or organic matter from the inorganic pigments present. The oxidising atmosphere data differ significantly from that of the inert atmosphere as the carbon-based pigments remain stable in the inert atmosphere.

The TG/DTG data show evidence of the presence of three regions of decomposition and a region of dehydration (Tables 1, 2). Dehydration is observed up to 140 °C. The first decomposition step, Step I, is observed in the region 140–400 °C. This region of decomposition is normally associated with the decomposition of iron hydroxides [13, 14]. The second decomposition step, Step II, is observed in the region 400–700 °C. This step with a DTG peak in the region 490–510 °C is associated with the dehydroxylation of kaolinite resulting in the formation of metakaolin [15]. The final mass loss step, Step III, is observed only in the argon atmosphere above 700 °C and is likely to be associated with the slow decomposition of organic matter which is otherwise oxidised in the air atmosphere below 700 °C and is, therefore, not observed.

The DSC data for an air atmosphere (Fig. 8) show exothermic behaviour in Step I for all specimens and is consistent with the oxidation of carbon containing matter. The exotherm is absent from the DSC data under an argon atmosphere (Fig. 9) suggesting that the carbonaceous material is oxidised in air, but is stable in this temperature range in an argon atmosphere. This observation is consistent with a charcoal rather than organic matter such as oils or polymer resin materials. Step II shows a characteristic

Table 1 DTG peak positions and decomposition ranges in °C for paint decomposition in an air atmosphere

Mass loss region	Black pigment	Brown pigment	Pink pigment	Cream pigment
Molecular water loss				
Range	RT–110	RT–120	RT–120	RT–100
Peaks	48	48	57	42
Step I: Decomposition of iron oxide hydroxides and charcoal oxidation				
Range	190–370	190–410	220–420	200–411
Peaks	260	265	256	257
	313	312	311	314
		364	354	350
			388	
Step II: Dehydroxylation of kaolinite to metakaolin				
Range	370–630	410–620	420–620	411–630
Peaks	498	495	514	500

Table 2 DTG peak positions and decomposition ranges in °C for paint decomposition in an argon atmosphere

Mass loss region	Black pigment	Brown pigment	Pink pigment	Cream pigment
Molecular water loss				
Range	RT–140	RT–145	RT–144	RT–144
Peaks	50	54	56	40
Step I: Decomposition of iron oxide hydroxides and some charcoal oxidation due to presence of 10 ppm O_2				
Range	140–392	145–395	144–371	144–374
Peaks	167	163	166	163
	186	188	185	184
	208	218	274	262
	264	273	347	286
	285	343	383	314
	306	388		344
	345			387
	382			
Step II: Dehydroxylation of kaolinite to metakaolin				
Range	392–655	395–654	371–680	374–678
Peaks	496	497	511	494
Step III: Further decomposition of charcoal				
Range	>760	>770	>860	>790
Mullite crystallisation				
Exotherm	920	908	915	921

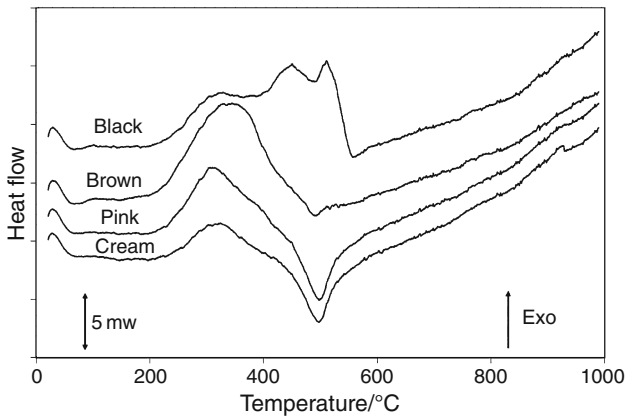

Fig. 8 DSC of paint specimens in an air atmosphere

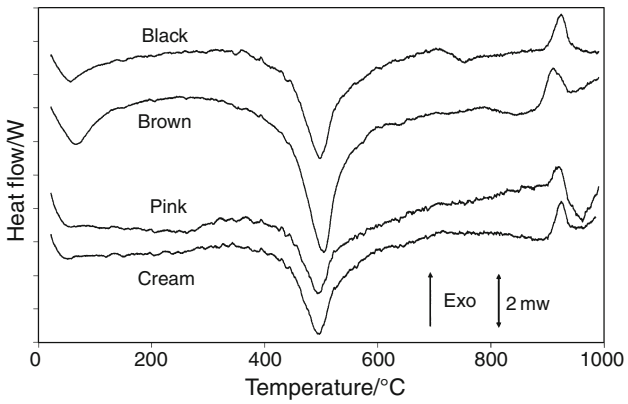

Fig. 9 DSC of paint specimens in an argon atmosphere

endotherm for the dehydroxylation of the kaolinite present in all pigments in both the air and argon atmospheres. This endotherm is superimposed with a broad exotherm in the brown and black pigments in the air atmosphere. Step II in the argon atmosphere only shows the dehydroxylation of the kaolinite. Step III is also evident in the heat flow data in the argon atmosphere for the brown and black pigments as endothermic behaviour above 700 °C.

Further differentiation of the components undergoing thermal decomposition can be attained by EVA. In this study, EVA was carried out using MS. A series of mass to charge ratios were used: 12 and 44 amu to identify the presence of CO_2, 17 and 18 amu to identify the presence of water, 30 amu for NO, 32 amu for O_2, 48 and 64 amu for SO_2, and 54, 64, 66, 67, 70, 72, 78, 81, and 91 amu as characteristic decomposition peaks of organic matter [16].

The presence of organic matter was discounted by the lack of observation of any peaks in the 54, 64, 66, 67, 70, 72, 78, 81, and 91 amu curves for each paint. Sulphur was not observed in the paints as no peaks in the SO_2 (48 and 64 amu) curves were observed. CO_2 was, however, observed in both the air (Fig. 10) and the argon (Fig. 11) atmospheres, indicating that oxidisable carbon is present. The observation of the presence of CO_2 in the argon

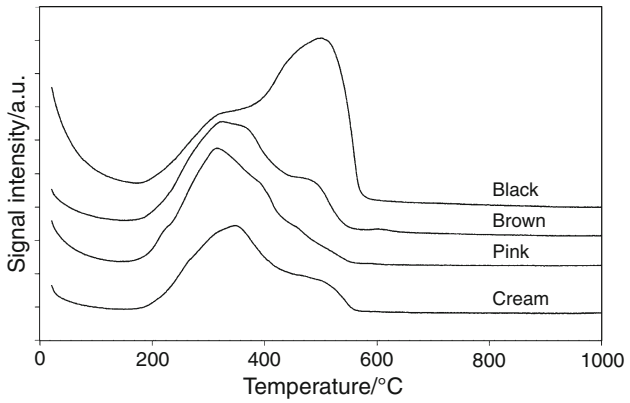

Fig. 10 44 amu mass spectra data for paint specimens in an air atmosphere

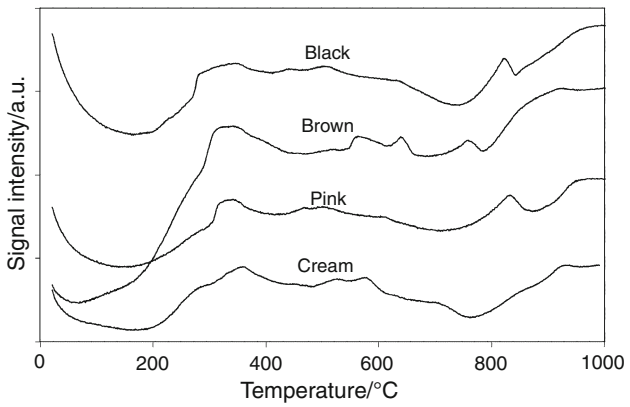

Fig. 11 44 amu mass spectra data for paint specimens in an argon atmosphere

atmosphere is due to the presence of oxygen (although small, <10 ppm) in the high purity argon used as a purge gas. The oxidation of the carbon present was also observable in the oxygen (32 amu) curve through the presence of negative peaks (depletion of O_2 in the oxidation of the charcoal) and correlated well with the peaks observed in the CO_2 curves during the decomposition in an air atmosphere. The oxidation of the carbon in the argon atmosphere was observed to be erratic and peaks did not correlate well with the DTG curves suggesting volatilisation of the carbon followed by subsequent gas phase reactions.

Water was observed in Step I for the cream and pink paints, but not for the brown and black paints in the air atmosphere. This is due either to the presence of hydrated salts (e.g., goethite) in the cream and pink paints or to residual water in the furnace swamping the detectable peaks in the brown and black. Water was detected in the evolved gas for all the paints in Step II, correlating with the dehydroxylation of the kaolinite.

Discussion

Based on each of the techniques used in the characterisation of the paints, three components were identified: charcoal, kaolinite, and quartz. Some evidence for the presence of haematite (rather than goethite due to the lack of water evolution in Step I) was also forthcoming from the XRD data. Based on the mass loss data, a crude measure of the composition may be made (Table 3). The proportion of kaolinite can be estimated from the TG mass loss in Step II in the argon atmosphere by assuming that the decomposition is stoichiometric according to:

$$\underset{\text{kaolinite}}{Al_2O_3 \cdot 2SiO_2 \cdot 2H_2O} \rightarrow \underset{\text{metakaolin}}{Al_2O_3 \cdot 2SiO_2} + 2H_2O$$

corresponding to a theoretical mass loss of 13.96% and assuming that the charcoal is inert in the argon atmosphere. This is a close approximation, but is clearly not true as some mass loss is associated with the oxidation of the carbon with the oxygen (<10 ppm) present in the high

Table 3 Mass losses and predicted compositions from thermal analysis

Atmosphere	Step	Black pigment	Brown pigment	Pink pigment	Cream pigment
Argon	Water loss <140 °C	1.8	1.5	1.2	1.2
	Step I 140–400 °C	5.8	4.7	4.4	3.9
	Step II 400–700 °C	15.0	14.6	14.3	14.0
	Step III >700 °C	1.8	1.5	1.2	1.2
Air	Water loss <140 °C	2.1	1.8	1.6	1.4
	Step I 140–400 °C	10.4	7.3	7.9	6.7
	Step II 400–700 °C	18.9	24.5	17.3	15.8
	Step III >700 °C	–	–	–	–
% Kaolinite		66.6	70.9	70.8	72.5
% Charcoal		3.6	9.6	2.6	1.6
% Residual		29.8	19.6	26.6	25.9

purity argon. Similarly, if it is assumed that all the charcoal is fully oxidised in the air atmosphere, the difference in mass loss between the air and the argon atmospheres can be attributed to the oxidation of the charcoal. As some oxidation of the charcoal does occur in the argon atmosphere, the proportion of kaolinite is overestimated, while the proportion of charcoal is underestimated. Creagh [4] determined the composition of typical white pigment to be 74% kaolinite, 18% quartz, 2% talc, 3% muscovite, and 3% other compounds. Talc and muscovite were not identified in the XRD patterns of the pigments investigated in this study, although the small proportions quoted are close to the limit of detection in XRD and so cannot be discounted. These proportions correlate very well with the proportions listed in Table 3 suggesting that this method of estimation works reasonably well.

Conclusions

TG in combination with DSC and MS has been used to investigate the composition of four ochre paint specimens of different appearance taken from an Australian bark painting. This approach has successfully identified the presence of both inorganic and organic components by carrying out the analyses in both oxidising and non-oxidising atmospheres. The main components of each paint specimen were determined to be kaolinite, quartz and charcoal. The percentage compositions of the main components were estimated based on mass losses determined using thermal analysis. Infrared spectra and XRD data recorded for the same paint specimens confirm the presence of the main components determined using thermal methods.

This study has demonstrated the potential of thermal methods for the characterisation of ochre paints. Valuable quantitative information using just milligram quantities of paint can be obtained using this approach. There is scope with thermal analysis to provide greater discrimination of pigments based upon an examination of the decomposition processes observed. By combining the use of thermal analysis with other analytical techniques including FTIR spectroscopy and XRD, it is possible to obtain valuable information about paint pigments.

References

1. Perkins H, West M, editors. One sun one moon: aboriginal art in Australia. Sydney: Art Gallery of New South Wales; 2007.
2. Creagh DC, Kubik ME, Sterns M. One the feasibility of establishing the provenance of Australian Aboriginal artefacts using synchrotron radiation X-ray diffraction and proton induced X-ray emission. Nucl Instrum Methods Phys Res A. 2007;580:721–4.
3. O'Neill PM, Creagh DC, Sterns M. Studies of the composition of pigments used traditionally in Australian Aboriginal bark paintings. Radiat Phys Chem. 2004;71:841–2.
4. Creagh DC. The characterisation of artefacts of cultural heritage significance using physical techniques. Radiat Phys Chem. 2005;74:426–42.
5. Creagh D, Lee A, Otieno-Alego V, Kubik M. Recent and future developments in the use of radiation for the study of objects of cultural heritage significance. Radiat Phys Chem. 2009;78:367–74.
6. Creagh DC, Otieno-Alego V. The use of radiation for the study of material of cultural heritage significance. Nucl Instrum Methods Phys Res B. 2004;213:670–6.
7. Madejova J. FTIR techniques in clay mineral studies. Vib Spectrosc. 2003;31:1–10.
8. Genestar C, Pons C. Earth pigments in painting: characterisation and differentiation by means of FTIR spectroscopy and SEM-EDS microanalysis. Anal Bioanal Chem. 2005;382:269–74.
9. Ip KH, Stuart BH, Ray AS, Thomas PS. A spectroscopic investigation of the weathering of a heritage Sydney sandstone. Spectrochim Acta A. 2008;71:1032–5.
10. Cornell RM, Schwertmann U. The iron oxides: structures, properties, reactions, occurrences and uses. Weinheim: Wiley-VCH; 2003.
11. Bertraux J, Frohlich F, Ildefonse P. Multicomponent analysis of FTIR spectra: quantification of amorphous and crystallized mineral phases in synthetic and natural sediments. J Sediment Res. 1998;68:440–7.
12. Guo Y, Bustin RM. FTIR spectroscopy and reflectance of modern charcoals and fungal decayed woods: implications for studies of inertinite in coals. Int J Coal Geol. 1998;37:29–53.
13. Genestar Julia C, Pons Bonafe C. The use of natural earths in picture: study and differentiation by thermal analysis. Thermochim Acta. 2004;413:185–92.
14. Frost RL, Ding Z, Ruan HD. Thermal analysis of goethite: relevance to Australian indigenous art. J Therm Anal Calorim. 2003;71:783–97.
15. Dweck J. Qualitative and quantitative characterization of Brazilian natural and organophilic clays by thermal analysis. J Therm Anal Calorim. 2008;92:129–35.
16. Onishi A, Thomas PS, Stuart BH, Guerbois JP, Forbes S. TG-MS characterisation of pig bone in an inert atmosphere. J Therm Anal Calorim. 2007;88:405–9.